Bisphenol S moderately decreases the expression of syncytiotrophoblast marker genes and induces apoptosis in human trophoblast lineages

Enoch Appiah Adu-Gyamfi[1], Joudi Salamah[1], Elisha Ann Cheeran[1], Bum-Kyu Lee[1*]

[1] Department of Biomedical Sciences, Cancer Research Center, University at Albany, State University of New York, Rensselaer, NY, 12144, USA

* Corresponding Author:
Email: blee6@albany.edu, phone: (518)-591-7231

Abstract

Bisphenol S (BPS) is currently used in the manufacturing of several household equipment such as water pipes and food containers. Hence, its entrance into the human body is almost inevitable. The presence of BPS in body fluids has been reported. However, its potential toxicity, especially on human placenta development and pregnancy progression, has not been explored. In this study, we assessed the impacts of BPS on self-renewal and differentiation potentials of placental stem cells, also known as trophoblast stem cells (TSCs), by exposing them to three different BPS concentrations during both self-renewal and differentiation of TSCs into syncytiotrophoblast (ST), extravillous trophoblast (EVT), and trophoblast organoids. Interestingly, BPS treatment did not affect the stemness, cell cycle and proliferation of the TSCs but it induced apoptosis in each trophoblast lineage. BPS altered the expression of several fusion-related genes. However, this alteration did not translate into significant morphological defects in the STs and organoids. Moreover, BPS did not impair the differentiation of TSCs into EVTs. These findings suggest that the presence of BPS at the feto-maternal interface may exaggerate trophoblast apoptosis and moderately inhibit the trophoblast fusion pathway to affect placenta development and pregnancy. Our study offers valuable insights into the potential toxicity of BPS on human placenta development, emphasizing the need for epidemiological assessment of the relationship between maternal serum levels of BPS and pregnancy complications.

Keywords: Bisphenol S, Placenta, Trophoblast, Proliferation, Differentiation, Apoptosis

1. Introduction

The human placenta is a transient organ that is indispensable for pregnancy progression and maternal health. The major cell type in the placenta is the trophoblast, which has three main lineages: cytotrophoblasts (CTs), syncytiotrophoblasts (STs) and extravillous trophoblasts (EVTs). During placenta development, the CTs, which are stem cells, proliferate and differentiate into the STs and EVTs, with a continuous occurrence of strictly controlled apoptosis to remove superfluous and dysfunctional cells (Adu-Gyamfi et al., 2021; Knöfler et al., 2019). While the EVTs invade the uterus to establish the uteroplacental circulation and the histotrophic nutrition, the STs serve as a barrier that controls the exchange of substances between the fetus and the mother (Adu-Gyamfi et al., 2021; Knöfler et al., 2019). It has been found that abnormal proliferation, differentiation, and apoptosis of the trophoblasts lead to defective placenta and pregnancy complications such as miscarriage, preeclampsia, and fetal growth restriction (Adu-Gyamfi et al., 2020b; Adu-Gyamfi et al., 2019; Erel et al., 2001; Farah et al., 2020; He et al., 2013; Sharp et al., 2010; Zhang et al., 2020). Accumulation of xenobiotics at the feto-maternal interface is believed to be among the contributing factors to these anomalies.

Some xenobiotics can compromise or exaggerate the functionality of several cells, tissues, and organs. One group of these chemicals is the bisphenols, among which are bisphenol A (BPA) and bisphenol S (BPS). BPA is used in the production of food and beverage containers, water pipes, medical equipment, coatings, adhesives, high-performance composites, and automotive and aircraft parts (Adu-Gyamfi et al., 2022). Ever since it was shown that BPA significantly affects several developmental processes, such as impairing decidualization (Nelson et al., 2020), inducing abnormal placentation, and causing pregnancy complications (Adu-Gyamfi et al., 2022), its use has been banned in some geographical settings. BPS has now been recommended as an alternative substitute for BPA. Hence, this chemical is currently used in the production of several equipment which were previously produced with BPA. Due to this, human exposure to this chemical is now on the rise. Contemporary evidence suggests that BPS is detectable in the follicular fluid (Žalmanová et al., 2023), blood, and urine (Jin et al., 2018; Smarr et al., 2018), raising concerns about its potential toxicity. Therefore, it is imperative to conduct a comprehensive examination of the potential toxic effects of this chemical to ascertain whether it is safe to the human body and pregnancy. It has been demonstrated that BPS affects EGF signaling in human trophoblast cells (Ticiani et al., 2022), impairs endocrine functions in the sheep placenta (Gingrich et al., 2018), and induces morphological defects in the junctional zone of the mouse placenta (Mao et al., 2020). However, the impacts of BPS on human placenta development remains to be clarified.

93 Previous research about the effects of xenobiotics on placenta development primarily relied on animal
94 models and immortalized or choriocarcinoma trophoblast cell lines such as JEG3, Bewo and HTR8/SVneo
95 cells. These models exhibit varying gene expression signatures and do not closely mirror human placenta
96 development. Therefore, experimental findings from them are not directly applicable to humans (Abbas et
97 al., 2020; Hemberger et al., 2020). Since it is unethical to administer xenobiotics to pregnant women, it
98 would be ideal to use an in vitro model that closely mirrors the human placental micro-environment for
99 studying the toxic effects of xenobiotics on placenta development. The use of human trophoblast stem cells
100 (TSCs) has been recommended in that regard (Adu-Gyamfi et al., 2022). The TSCs have the ability to
101 differentiate into trophoblast lineages that have morphological characteristics and transcriptomic signatures
102 which closely resemble those of the early human placenta (Okae et al., 2018). Therefore, they serve as a
103 better model for studying the mechanisms of early human placenta development.
104
105 In this study, we aimed to determine the impacts of BPS on trophoblast stemness, cell cycle, proliferation,
106 differentiation, and apoptosis. We differentiated human TSCs (which are the in vitro counterparts of the
107 CTs) into STs, EVTs, and organoids in the presence or absence of BPS and then assessed the effects. Our
108 findings will contribute to policy formulation regarding BPS use.
109
110 **2. Materials and methods**
111
112 **2.1 TSC culture**
113 Human TSCs were grown in TSC culture medium [Dulbecco's modified Eagle's medium (DMEM)/F12
114 (Gibco), New York, USA] supplemented with 0.2% fetal bovine serum (FBS; GeminiBio, California,
115 USA), 1% insulin-transferrin-selenium-ethanolamine (ITS-X; Gibco), 0.1 mM β-mercaptoethanol (Sigma-
116 Aldrich, St Louis, Washington, USA), 0.3% bovine serum albumin (BSA; GeminiBio), 0.5% penicillin–
117 streptomycin (Gibco), 0.5 μM A83-01 (Wako Pure Chemical Corporation, Osaka, Japan), 0.5 μM
118 CHIR99021 (Selleck Chemicals, Texas, USA), 0.5 μM SB431542 (Stemcell Technologies, Washington,
119 USA), 0.8 mM valproic acid (VPA; Wako Pure Chemical Corporation), 5 μM Y27632 (ROCK inhibitor,
120 Selleck Chemicals), 1.5 μg/ml L-ascorbic acid (Sigma-Aldrich) and 50 ng/ml epidermal growth factor
121 (EGF; PeproTech, Cranbury, New Jersey, USA) in accordance with a previous protocol (Okae et al., 2018).
122 Cell culture plates that had been coated with 5 μg/ml of Collagen IV (Corning, Bedford, Massachusetts,
123 USA) were used for the cell culture. On reaching 70–80% confluency, the cells were detached with TrypLE
124 (Gibco) for 8 min at 37°C and then passaged at a 1:3 split ratio. TSCs were cultured in a 37°C and 5%
125 CO_2 incubator. The medium was replaced every day with a fresh medium.
126

127 **2.2 Differentiation of TSCs to STs**

128 Previously cultured TSCs at ~80% confluence were trypsinized. 3×10^5 of the TSCs were seeded in 6 cm
129 Petri dishes and cultured in 3 mL of ST medium [DMEM/F12 supplemented with 2 μM forskolin, 0.3%
130 BSA, 1% ITS-X supplement, 0.1 mM 2-mercaptoethanol, 4% KSR, 50 ng/ml EGF, 0.5% Penicillin-
131 Streptomycin, and 2.5 μM Y27632] in accordance with a previous protocol (Okae et al., 2018). On the
132 second and fourth days, the medium was replaced with a fresh medium. On the 5th day, the STs were
133 collected, and washed to remove dead cells after which RNA and proteins were extracted from them.

134

135 **2.3 Differentiation of TSCs to EVTs**

136 Trypsinized TSCs were seeded in 6-well plates pre-coated with 1 μg/ml of Collagen IV at a density of $1 \times$
137 10^5 cells per well and grown in 2 mL of EVT medium [DMEM/F12 supplemented with 0.3% BSA, 0.1 mM
138 2-mercaptoethanol, 4% KSR, 0.5% Penicillin-Streptomycin, 1% ITS-X supplement, 2.5 μM Y27632,
139 100 ng/ml NRG1, and 7.5 μM A83-01] in accordance with a previous protocol (Okae et al., 2018). Shortly
140 after suspending the cells in the medium, Matrigel (Corning, Bedford, Massachusetts, USA) was added to
141 a final concentration of 2%. On day 3, the medium was replaced with EVT medium without NRG1, and
142 Matrigel was added to a final concentration of 0.5%. On day 6, the medium was replaced with EVT medium
143 without NRG1 and KSR. Matrigel was then added to a final concentration of 0.5%. The cells were harvested
144 on day 8 for further experiments.

145

146 **2.4 Differentiation of TSCs to organoids**

147 TSCs at ~80% confluence were trysinized. 5 x 10^3 TSCs were suspended in 50 μL of 72% Matrigel droplet
148 in Advanced DMEM/F12 medium. 5 droplets of the cell-matrigel mixture were introduced into the middle
149 of 6 cm Petri dishes. It was ensured that the droplets were separated from one another and never adhered to
150 the walls of the Petri dishes. The droplets were polymerized by putting the Petri dishes in a humidified 5%
151 CO_2 incubator at 37 ^{O}C for 30 mins. The Petri dishes were then removed from the incubator, and then 2ml
152 of trophoblast organoid medium was added to the droplets and the Petri dishes put back in the incubator.
153 The medium was replaced every 2 days. The culture was continuously monitored for the appearance of
154 small organoid clusters. On day 8, the organoids were harvested, and total RNA and proteins were extracted
155 from them. The trophoblast organoid medium comprised Advanced DMEM/F12 supplemented with N2,
156 B27, 2 mM L-glutamine, 100 ng/mL Recombinant human FGF-2, 500 nM A83-01, 1.5 μM CHIR99021,
157 50 ng/mL Recombinant human EGF, 1.25 mM N-Acetyl-L-cysteine, 50 ng/mL Recombinant human HGF,
158 100 μg/mL Primocin, 80 ng/mL Recombinant human R-spondin-1, 2.5 μM Prostaglandin E2, and 2 μM Y-
159 27632, same as the medium that was used in a previous study in which organoids were established from
160 human primary trophoblast cells (Turco et al., 2018).

161

162 **2.5 Treatment of the TSCs, STs, EVTs, and organoids with BPS**

163 BPS (Sigma-Aldrich, CAS-No:80-09-1, Purity: 98%) was dissolved in absolute ethanol, and then
164 transferred into cell culture media to yield final concentrations of 0.01, 0.1 and 1 μM, which are
165 concentrations that lie within the reported urine and blood levels of BPS in humans (Hehn, 2016; Jin et al.,
166 2018; Smarr et al., 2018). Since TSCs, STs, EVTs, and organoids grow and develop in special media,
167 specific BPS-containing media and their negative controls (NCs) were prepared for each model. The TSCs
168 were treated with the various BPS concentrations for 2 days and were then harvested for cell cycle analysis,
169 apoptosis assessment, and total RNA extraction. Differentiation of the TSCs into STs, EVTs, and organoids
170 was done as already described above, with the only modification being the addition of BPS and ethanol to
171 the media. On day 5, the STs were harvested, and on day 8, the EVTs and organoids were harvested for
172 subsequent experiments.

173

174 **2.6 Cell proliferation assay**

175 The CCK8 kit (Abcam, Cambridge, Massachusetts, USA) was used to assess the proliferative rate of the
176 TSCs. 3×10^3 cells were seeded in 96-well plates in triplicates. After treating the TSCs with 0.01, 0.1 and
177 1μM of BPS and the NCs for 1 day, 2 days or 3 days in 100ul of media per well, we added 10 μl of the
178 CCK8 solution to each well, and then incubated the cells for 1 h at 37 ◦C. We measured the optical density
179 at 450 nm with a microplate reader (Thermo Fisher Scientific, MA, USA).

180

181 **2.7 Flow cytometric analysis of the cell cycle and apoptosis**

182 Only TSCs were used for cell cycle analysis while both TSCs and EVTs were used for the apoptosis assay.
183 The cells were trypsinized and washed. For cell cycle analysis, about $1x10^5$ TSCs were fixed with 70%
184 ethanol and incubated for, at least, 3 h at -20ºC. After removing the ethanol, 150ul of Muse Cell Cycle
185 reagent (Millipore, MCH100106) was used to incubate the cells for 30 mis at room temperature in the dark.
186 The cells were analyzed by using the Muse flow cytometer. For apoptosis assay, about $1x10^5$ TSCs or EVTs
187 were incubated with 150ul of Muse Annexin V & Dead Cell reagent (Millipore, MCH100105) for 20 mins
188 at room temperature in the dark. The cells were then analyzed with the Muse flow cytometer (Luminex,
189 Watertown, Massachusetts, USA).

190

191 **2.8 Total RNA extraction and RT-qPCR**

192 Total RNA was extracted from the TSCs, STs, EVTs and the organoids by using the single cell RNA
193 purification kit (Norgen Biotek Corp, 51800, Ontario, Canada). The quality of the RNA was evaluated with
194 1% agarose gel electrophoresis and UV spectrophotometry. Complementary DNAs (cDNAs) were

generated from 300 ng of total RNA using the SuperScript™ III first strand synthesis SuperMix kit (Thermo Fisher Scientific, 18080400) and then diluted 20 times with DNase-free water. RT-qPCR was carried out by using the PowerTrack™ SYBR Green Master Mix (Thermo Fisher Scientific, A46110). Primers were designed to amplify the junction between two exons using a web-based primer design program, Primer 3 (http://bioinfo.ut.ee/primer3/). The primer sequences are listed in Supplementary Table 1. Cycle threshold (Ct) values of the samples and the controls were normalized against GAPDH while the relative gene expression was calculated as fold enrichment by using the $2^{-\Delta\Delta CT}$ method. The relative gene expression was calculated from an average of at least two replicates.

2.9 Protein extraction and Western blot

4X Laemmli sample buffer (Bio-Rad, USA) supplemented with 2-Mercaptoethanol was added to the STs or organoids, and the mixture homogenized. The mixtures were incubated at 90 ◦C for 10 min, after which appropriate concentrations of SDS-PAGE gel were prepared and used for electrophoresis. The proteins in the gels were transferred to PVDF membranes (Bio-Rad, USA). The non-specific binding sites on the membranes were blocked with 5% non-fat skim milk (Foodhold, USA) at 25 ◦C for 60 min. The membranes were then probed with primary antibodies at 4 ◦C for 16h. The primary antibodies were specific for SDC1, CGB3, CSH1, CDH1 and GAPDH (Santa Cruz, USA). For each primary antibody, the concentration used was 1 μg/ml. GAPDH was used as a control to ensure that protein loading was equal across the wells in the gels. After washing the membranes three times with PBST, we incubated them with HRP-conjugated goat anti-mouse IgG (0.5 μg/ml, Active Motif, USA) at 25 ◦C for 1 h. After this, the membranes were washed three times with PBST. Protein bands were then detected in the membranes by using the ECL chromogenic solution (Thermo Fisher Scientific, USA). The protein bands were quantified by using the ImageJ software.

2.10 Statistical analyses

The data were analyzed by using the GraphPad Prism 9 software. Error bars in the figures indicate mean ± SD (standard deviation) of, at least, two independent experiments. Significant differences between groups were assessed with two-tailed t-test. *, **, and *** denote significance levels of $P < 0.05$, $P < 0.01$, and $P < 0.001$, respectively.

3. Results

3.1. Successful establishment of the ST, EVT, and organoid models

We established in vitro models of the villous and extravillous trophoblasts of the human placenta by differentiating TSCs into STs, EVTs, and organoids (**Figs. 1A**). Each trophoblast lineage had morphological and gene expression characteristics that are comparable to those of the actual placenta. In the ST model, we

229 verified the upregulation of ST markers, including fusogenic genes (*CGA, CGB3, CSH1, ERVW1,*
230 *ERVFRD, GCM1, PSG1, SDC1,* and *CYP19A1*) (**Figs. 1B**, **1C,** and **1D)** as well as downregulation of
231 *TEAD4* (a stem cell marker) and *CDH1* (an epithelial marker) (**Fig. 1E**) compared to TSCs. In the EVT
232 model, we confirmed the upregulation of EVT markers (*HLA-G, MMP2, ASCL2, ITGA5,* and *FN1*) (**Fig.**
233 **1F**) and a decrease in *TEAD4* expression (**Fig. 1G**) compared to TSCs. In the organoid model, we observed
234 that the sizes of the organoids gradually increased during their 12 days formation period (**Fig. 1H**).
235 Interestingly, the expressions of *CGA, CGB3, GCM1, PSG1, SDC1, CSH1,* and *CYP19A1* increased
236 gradually and reached their maximal levels on day 8 of the organoid formation process and then declined
237 afterwards (**Fig 1I**), suggesting that the organoids probably reached their maximal maturation on day 8.
238 Hence, day 8 organoids were selected for further experiments. We further validated an increase in the
239 expressions of *CGA, CGB3, CSH1, ERVW1, ERVFRD, GCM1, PSG1, SDC1,* and *CYP19A1* in the day 8
240 organoids compared to the TSCs (**Figs. 1J, 1K,** and **1L**). Notably, while there was a reduction in the
241 expression of *CDH1*, there were no significant changes in the expressions of stem cell markers (*TEAD4,*
242 *ELF5, GATA3*, and *TP63*) (**Fig. 1M**) and proliferation markers (*Ki67* and *PCNA*) (**Fig. 1N**). This is likely
243 due to the organoids comprising a mixture of TSCs and STs. In summary, we successfully established in
244 vitro models representing both villous and extravillous trophoblasts of the human placenta.
245

246 **3.2**. **BPS elicits no significant effect on stemness, proliferation, and cell cycle of TSCs**

247 We exposed TSCs to three different BPS concentrations (0.01, 0.1, and 1 μM) for 2 days, as illustrated in
248 **Fig. 2A**. We observed that BPS treatment did not affect the expressions of stem cell marker genes (**Fig.**
249 **2B**). Consistently, proliferation assay showed no difference in growth rates between the BPS-treated and
250 the NC TSCs (**Fig. 2C**), along with no significant expression change in proliferation marker genes (**Fig.**
251 **2D**). Flow cytometric analysis further indicated that the cell cycle did not differ between the BPS-treated
252 and the NC TSCs (**Fig. 2E** and **Supplementary Fig. 1**). We also assessed the impact of each BPS
253 concentration on the proliferation and stemness of the TSCs within the organoids. On day 8 of TSC
254 differentiation into the organoids, we found that BPS treatment did not affect the expressions of the stem
255 cell markers as well as the cell proliferation markers within the organoids (**Figs. 2F** and **2G**). Collectively,
256 these results indicate that BPS has no significant effect on the self-renewal of TSCs.
257

258 **3.3. BPS moderately decreases the expression of ST marker genes in STs and organoids, while having**
259 **no discernible effect on EVT formation**

260 To explore the impacts of BPS on the multipotency of TSCs, we treated the TSCs with three different BPS
261 concentrations (0.01, 0.1, and 1 μM) during differentiation of TSCs into STs, EVTs, and organoids (**Figs.**
262 **3A** and **4B**). On day 5 of ST formation, we observed no significant morphological differences between the

263 BPS-treated STs and their corresponding NC STs (**Fig. 3A**). However, BPS treatment moderately reduced
264 the expressions of several ST marker genes. For instance, in the STs treated with 0.01 μM of BPS, *CGB3,*
265 *CSH1, GCM1,* and *PSG1* were downregulated while *CDH1* and *TEAD4* were upregulated. However, the
266 expressions of *CGA, ERVW1, ERVFRD,* and *CYP19A1* remained unchanged compared to the NCs (**Fig.**
267 **3B**). Importantly, in the STs treated with 0.1 and 1 μM of BPS, we observed that 8 out of 9 ST marker
268 genes (*CGA, CGB3, CSH1, ERVW1, GCM1, PSG1, SDC1* and *CYP19A1*) were downregulated while *CDH1*
269 and *TEAD4* were upregulated compared to the NCs (**Fig. 3B**). This suggests that higher concentrations of
270 BPS have stronger impacts on the downregulation of ST marker genes. Consistent with this, 1 μM of BPS
271 moderately decreased the protein levels of CGB3, CSH1, and SDC1 while increasing the protein levels of
272 CDH1 (**Fig. 3C** and **Fig. 3D**). Just like the STs, the organoids treated with BPS showed no significant
273 change in morphology (**Fig. 3E**). However, a reduction in multiple ST marker genes was evident in this
274 group compared to the NCs. These genes include *CGA, CGB3, CSH1, GCM1, ERVFRD, SDC1,* and
275 *CYP19A* (**Fig. 3F**). Decreased protein levels of SDC1 and increased protein levels of CDH1 were also found
276 in the organoids treated with 1μM of BPS (**Fig. 3G** and **3H**). On day 8 of TSC differentiation into EVTs,
277 the BPS-treated EVTs and their corresponding NCs did not show significant morphological differences or
278 changes in the expression of EVT marker genes (**Figs. 4A** and **4B**). Taken together, these findings suggest
279 that BPS moderately inhibits the induction of ST marker genes during ST formation, while eliciting no
280 effect on EVT formation.
281
282 **3.4. BPS induces apoptosis in trophoblast lineages**
283 We determined the impacts of 0.01, 0.1 and 1 μM of BPS on the apoptosis of TSCs. Additionally, during
284 the differentiation of TSCs into the STs, EVTs, and organoids, we assessed the impacts of these three
285 different BPS concentrations on apoptosis in each trophoblast model. In the TSCs, we found that each BPS
286 concentration increased the proportion of early and total apoptotic cells in a dose-dependent manner
287 compared to the NC TSCs (**Fig. 5A** and **Supplementary Figs. 2** and **4A**). Additionally, we found an
288 increase in the expressions of the pro-apoptotic genes (*BAX, TP53*, and *CDKN1B*) in the TSCs treated with
289 each concentration of BPS (**Fig. 5B**). Treatment with BPS concentrations of 0.1 and 1 μM also resulted in
290 a reduction in the expressions of the anti-apoptotic genes in the TSCs. Particularly, treatment with 1 μM of
291 BPS significantly reduced the expression levels of *BCL2, SIRT1, MCL1, and PTMA* compared to the NC
292 TSCs (**Fig. 5B**). In the EVTs, we found that only 1 μM of BPS induced apoptosis (**Fig. 5C** and
293 **Supplementary Figs. 3** and **4B**), leading to an increase in the proportion of late and total apoptotic cells
294 compared to the NC EVTs. Further assessment showed that *BAX, TP53,* and *CDKN1B* were upregulated
295 while *BCL2* was downregulated in the EVTs treated with 1 μM of BPS (**Fig. 5D**). However, unlike TSCs,
296 the EVTs treated with 1μM of BPS did not show any change in the expressions of *SIRT1, MCL1,* and *PTMA*

297 compared to the NC EVTs (**Fig. 5D**). In the ST model, 0.01 μM of BPS did not affect the expressions of
298 the apoptosis markers. However, 0.1 and 1 μM of BPS were able to reduce the expressions of anti-apoptotic
299 genes (*BCL2, SIRT1,* and *MCL1*) although they had no effect on the expressions of pro-apoptotic genes
300 (**Fig. 5E**). In the organoid model, only the 1μM of BPS was able to downregulate *BCL2, SIRT1,* and *MCL1*
301 while upregulating *TP53* and *CDKN1B*. However, it did not affect the expressions of *PTMA* and *BAX* (**Fig.**
302 **5F**). These findings suggest that BPS can induce apoptosis in trophoblast lineages in a dose-dependent
303 manner.
304
305 **4. Discussion**
306 In this study, we successfully established in vitro human placental models. In these models, the TSCs
307 organized into either villous or extravillous structures that are similar to those of the actual placenta. Human
308 placenta development mainly encompasses trophoblast proliferation, differentiation, and apoptosis which
309 are critically regulated by a myriad of molecules, including transcription factors (Papuchova and Latos,
310 2022), hormones (Adu-Gyamfi et al., 2020c), and cytokines (Adu-Gyamfi et al., 2020a; Appiah Adu-
311 Gyamfi et al., 2020). During differentiation, the CTs either transform into STs or EVTs. Formation of the
312 STs, a process known as syncytialization, involves the fusion of the cell membranes of adjacent CTs,
313 leading to protoplasmic merging (Kar et al., 2007). This occurrence is mediated by molecular processes
314 such as upregulation of the syncytins (ERVW1, ERVFRD) (Roberts et al., 2021) and the hormonal genes
315 (CGA, CGB3) (Okae et al., 2018) as well as the downregulation of epithelial markers such as CDH1 (E-
316 cadherin) (Adu-Gyamfi et al., 2021). We confirmed these patterns of gene expression upon differentiation
317 of TSCs into STs and organoids, providing evidence that we successfully established ST and trophoblast
318 organoid models. Formation of the EVTs, a process known as epithelial-mesenchymal transition, is
319 characterized by the CTs acquiring a spindle-shaped morphology and invasive abilities. This cellular
320 process is mediated by the upregulation of HLA-G and mesenchymal markers such as ASCL2, MMP2, and
321 ITGA5 (Okae et al., 2018; Varberg et al., 2021). As expected, we observed this expression pattern of the
322 molecular markers in the EVT lineage we established. By using these models, we have demonstrated that
323 BPS may moderately interfere with placenta development.
324
325 Proliferation of the CTs is the first stage in human placenta development. Both hypo- and hyper-
326 proliferative rates of trophoblast cells are detrimental to the formation of a functional placenta. For instance,
327 when CT proliferation is reduced, few CTs become available to undergo differentiation, leading to defective
328 ST and EVT formation. Conversely, when proliferation is excessively stimulated, CT differentiation
329 becomes inhibited, resulting in the impairment of ST and EVT formation. A previous study demonstrated
330 that BPS does not affect the proliferation of HTR8/SVneo cells (Ticiani et al., 2022). This cell line is

331 immortalized and has characteristics of the non-proliferative extravillous trophoblast cells which are
332 completely different from the progenitor CTs or TSCs. By using TSCs and organoid models, we have
333 shown that BPS does not affect the proliferation, cell cycle, and stemness of TSCs. Hence, BPS may not be
334 detrimental to the proliferation and renewal of the trophoblast progenitor cells within the placenta.
335
336 At the feto-maternal interface, physiologic regulation of trophoblast differentiation is vital to the
337 establishment of a normal placental architecture while dysregulation of this process, either due to the
338 abnormal expression of some genes or the presence of a xenobiotic, induces placental abnormalities to
339 affect pregnancy (Gong et al., 2021; Mohamad et al., 2020; Rosenfeld, 2021; Wu et al., 2023). In this study,
340 we found that BPS did not induce noticeable defects in EVT morphology and the expression of EVT marker
341 genes. We also found that BPS did not significantly affect the morphologies of the STs and organoids.
342 However, it moderately reduced the levels of several ST formation marker genes. Additionally, it
343 augmented the expression of the epithelial marker, *CDH1*, and the stem cell marker, *TEAD4* (Saha et al.,
344 2020) in STs. Notably, BPS elicited these effects in a dose-dependent manner, with the highest
345 concentration causing the most marked effect. Consistent with our observation, BPS impaired the placental
346 cell fusion pathway but it did not affect the morphology of the sheep placenta (Gingrich et al., 2018).
347 Similarly, in a previous in vitro study, ~0.8 μM of BPS did not affect the morphology of spontaneously
348 fused primary CTs (Ticiani et al., 2021). Collectively, these findings suggest that BPS may cause a moderate
349 molecular-level defect which does not translate into significant morphological defects in STs. Besides, BPS
350 may have no significant effect on CT differentiation into EVTs during placenta development.
351
352 Trophoblast apoptosis is an integral process in placenta development. The interplay between pro- and anti-
353 apoptotic regulators at the feto-maternal interface tightly regulates the rate of trophoblast apoptosis. During
354 normal pregnancy, trophoblast apoptosis increases with advancing gestation. This serves to eliminate
355 unwanted, superfluous, and dysfunctional cells; thereby, promoting placental growth and functionality.
356 However, excessive apoptosis impairs placenta development to cause pregnancy pathologies (Raguema et
357 al., 2020; Sharp et al., 2010; Straszewski-Chavez et al., 2005; Tomas et al., 2011). We have shown that
358 BPS triggers apoptosis in each trophoblast lineage. This was evidenced by an increase in the proportion of
359 total apoptotic TSCs and EVTs, an increase in the expression of pro-apoptotic genes and a reduction in the
360 expression of anti-apoptotic genes in the TSCs, STs, EVTs, and the organoid model. While all the
361 concentrations of BPS triggered apoptosis in the TSCs, only the higher BPS concentrations were able to
362 induce apoptosis in the STs and EVTs. This suggests that CTs may be more susceptible to the apoptotic
363 effects of BPS than STs and EVTs. Due to this apoptotic effect, the presence of BPS within the placental

micro-environment may have a synergistic effect with physiological apoptosis; thereby, amplifying trophoblast apoptosis to the detriment of placenta formation and functioning.

5. Conclusions

This study is the first to use human TSCs and trophoblast differentiation models to assess the impacts of BPS on human placenta development. Our findings suggest that the presence of BPS at the feto-maternal interface may exaggerate trophoblast apoptosis while moderately inhibiting trophoblast fusion to impair placenta development. Since BPS and its products are in use, the global consumption of BPS is bound to rise exponentially in the coming decades. Hence, epidemiological studies should monitor BPS levels in the blood and placentas of pregnant women and assess the relationship between maternal serum levels of BPS and pregnancy complications. The findings will assist in policy formulations concerning the use of BPS and its products in daily life.

Data Availability

The original data can be obtained from the corresponding author via an email.

Acknowledgement

We are grateful to Dr. Takahiro Arima and Dr. Hiroaki Okae of Tohoku University for providing us with human TSCs and technical advice. This research was supported by start-up funding from the University at Albany-State University of New York

Conflict of Interest

The authors have declared that they have no conflict of interest.

Figure legends

Fig. 1. The established placental models and their characteristics (**A**) Images showing the differentiation of TSCs into EVT, ST, and organoid models; (**B** and **C**) Expression fold changes of ST marker genes in STs relative to TSCs; (**D**) Protein levels of ST marker genes in TSCs and STs; (**E**) Transcript levels of epithelial (*CDH1*) and stem cell (*TEAD4*) markers in STs relative to TSCs; (**F**) Expression fold changes of EVT marker genes in EVTs relative to TSCs; (**G**) Transcript level of a stem cell marker, *TEAD4*, in EVTs relative to TSCs; (**H**) Images showing the time-course differentiation of TSCs into organoids; (**I**) Expression fold changes of ST marker genes during the time-course differentiation of TSCs into organoids; (**J** and **K**) Expression fold changes of ST marker genes in organoids relative to TSCs;

398 (**L**) Protein levels of ST marker genes in TSCs and organoids; (**M** and **N**) Transcript levels of stem cell
399 markers (**M**) and proliferation markers (**N**) in organoids relative to TSCs.
400
401 **Fig. 2. BPS does not affect TSC marker gene expression, cell cycle, and proliferation.** (**A**) A schematic
402 diagram illustrating the experimental design we used to investigate the impacts of BPS on the self-renewal
403 of TSCs and their differentiation potentials. We treated TSCs with BPS for 2 days. Also, during the
404 differentiation of TSCs into STs, EVTs, and organoids, we treated them with BPS (0.01, 0.1, or 1 μM). (**B**)
405 Transcript levels of stem cell markers in the BPS-treated TSCs relative to NCs; (**C**) Proliferation rates in
406 the BPS-treated and NC TSC; (**D**) Transcript levels of proliferation markers in the BPS-treated TSCs
407 relative to NCs; (**E**) Cell population distribution in different cell cycle phases in BPS-treated and NC TSCs.
408 (**F**) Transcript levels of stem cell markers in the BPS-treated organoids relative to NCs; (**G**) Transcript
409 levels of proliferation markers in the BPS-treated organoids relative to NCs.
410
411 **Fig. 3. BPS moderately decreases the expression of trophoblast fusion marker genes in the STs and**
412 **organoids.** (**A**) Representative images showing BPS-treated and NC STs after 5 days of TSC differentiation
413 into STs; (**B**) Transcript levels of trophoblast fusion, stem cell, and epithelial markers in the BPS-treated
414 STs relative to NC STs; (**C**) Protein levels of ST marker genes in the BPS-treated STs and NCs; (**D**) Protein
415 levels of ST marker genes in the BPS-treated STs relative to the NCs; (**E**) Representative images showing
416 BPS-treated and NC organoids after 8 days of TSC differentiation into organoids; (**F**) Transcript levels of
417 trophoblast fusion, stem cell, and epithelial markers in the BPS-treated organoids relative to NC organoids;
418 (**G**) Protein levels of ST marker genes in the BPS-treated organoids and NCs; (**H**) Protein levels of ST
419 marker genes in the BPS-treated organoids relative to the NCs
420
421 **Fig. 4. BPS does not affect EVT morphology and the expressions of EVT marker genes.** (**A**)
422 Representative images showing BPS-treated and NC EVTs after 8 days of TSC differentiation into EVTs;
423 (**B**) Transcript levels of EVT markers in the BPS-treated EVTs relative to NC EVTs.
424
425 **Fig. 5. BPS induces apoptosis in TSCs, STs, EVTs, and organoids.** (**A**) The distribution of cell
426 population in different apoptotic phases (EAC: Early apoptotic cells, LAC: late apoptotic cells, TAC: Total
427 apoptotic cells, and DC: Dead cells) of BPS-treated and NC TSCs; (**B**) Transcript levels of apoptosis
428 markers in the BPS-treated TSCs relative to NC TSCs; (**C**) The distribution of cell population in different
429 apoptotic phases of BPS-treated and NC EVTs; (**D**) Transcript levels of apoptosis markers in the 1uM BPS-
430 treated and NC EVTs; (**E**) Transcript levels of apoptosis markers in the BPS-treated STs relative to NC
431 STs; (**F**) Transcript levels of apoptosis markers in the BPS-treated organoids relative to NC organoids.

References

Abbas, Y., Turco, M.Y., Burton, G.J., Moffett, A., 2020. Investigation of human trophoblast invasion in vitro. Hum Reprod Update 26, 501-513.

Adu-Gyamfi, E.A., Czika, A., Gorleku, P.N., Ullah, A., Panhwar, Z., Ruan, L.L., Ding, Y.B., Wang, Y.X., 2021. The Involvement of Cell Adhesion Molecules, Tight Junctions, and Gap Junctions in Human Placentation. Reprod Sci 28, 305-320.

Adu-Gyamfi, E.A., Ding, Y.B., Wang, Y.X., 2020a. Regulation of placentation by the transforming growth factor beta superfamily†. Biol Reprod 102, 18-26.

Adu-Gyamfi, E.A., Fondjo, L.A., Owiredu, W.K.B.A., Czika, A., Nelson, W., Lamptey, J., Wang, Y.X., Ding, Y.B., 2020b. The role of adiponectin in placentation and preeclampsia. Cell Biochem Funct 38, 106-117.

Adu-Gyamfi, E.A., Lamptey, J., Duan, F., Wang, Y.X., Ding, Y.B., 2019. The transforming growth factor β superfamily as possible biomarkers of preeclampsia: a comprehensive review. Biomark Med 13, 1321-1330.

Adu-Gyamfi, E.A., Rosenfeld, C.S., Tuteja, G., 2022. The impact of bisphenol A on the placenta†. Biol Reprod 106, 826-834.

Adu-Gyamfi, E.A., Wang, Y.X., Ding, Y.B., 2020c. The interplay between thyroid hormones and the placenta: a comprehensive review†. Biol Reprod 102, 8-17.

Appiah Adu-Gyamfi, E., Tanam Djankpa, F., Nelson, W., Czika, A., Kumar Sah, S., Lamptey, J., Ding, Y.B., Wang, Y.X., 2020. Activin and inhibin signaling: From regulation of physiology to involvement in the pathology of the female reproductive system. Cytokine 133, 155105.

Erel, C.T., Dane, B., Calay, Z., Kaleli, S., Aydinli, K., 2001. Apoptosis in the placenta of pregnancies complicated with IUGR. Int J Gynaecol Obstet 73, 229-235.

Farah, O., Nguyen, C., Tekkatte, C., Parast, M.M., 2020. Trophoblast lineage-specific differentiation and associated alterations in preeclampsia and fetal growth restriction. Placenta 102, 4-9.

Gingrich, J., Pu, Y., Roberts, J., Karthikraj, R., Kannan, K., Ehrhardt, R., Veiga-Lopez, A., 2018. Gestational bisphenol S impairs placental endocrine function and the fusogenic trophoblast signaling pathway. Arch Toxicol 92, 1861-1876.

Gong, S., Gaccioli, F., Dopierala, J., Sovio, U., Cook, E., Volders, P.J., Martens, L., Kirk, P.D.W., Richardson, S., Smith, G.C.S., Charnock-Jones, D.S., 2021. The RNA landscape of the human placenta in health and disease. Nat Commun 12, 2639.

He, G., Xu, W., Chen, Y., Liu, X., Xi, M., 2013. Abnormal apoptosis of trophoblastic cells is related to the up-regulation of CYP11A gene in placenta of preeclampsia patients. PLoS One 8, e59609.

Hehn, R.S., 2016. NHANES Data Support Link between Handling of Thermal Paper Receipts and Increased Urinary Bisphenol A Excretion. Environ Sci Technol 50, 397-404.

Hemberger, M., Hanna, C.W., Dean, W., 2020. Mechanisms of early placental development in mouse and humans. Nat Rev Genet 21, 27-43.

Jin, H., Zhu, J., Chen, Z., Hong, Y., Cai, Z., 2018. Occurrence and Partitioning of Bisphenol Analogues in Adults' Blood from China. Environ Sci Technol 52, 812-820.

Kar, M., Ghosh, D., Sengupta, J., 2007. Molecular correlates of syncytialization in muscle and placenta. Indian J Physiol Pharmacol 51, 311-325.

Knöfler, M., Haider, S., Saleh, L., Pollheimer, J., Gamage, T.K.J.B., James, J., 2019. Human placenta and trophoblast development: key molecular mechanisms and model systems. Cell Mol Life Sci 76, 3479-3496.

Mao, J., Jain, A., Denslow, N.D., Nouri, M.Z., Chen, S., Wang, T., Zhu, N., Koh, J., Sarma, S.J., Sumner, B.W., Lei, Z., Sumner, L.W., Bivens, N.J., Roberts, R.M., Tuteja, G., Rosenfeld, C.S., 2020. Bisphenol A and bisphenol S disruptions of the mouse placenta and potential effects on the placenta-brain axis. Proc Natl Acad Sci U S A 117, 4642-4652.

480 Mohamad, M.A., Mohd Manzor, N.F., Zulkifli, N.F., Zainal, N., Hayati, A.R., Ahmad Asnawi, A.W., 2020.
481 A Review of Candidate Genes and Pathways in Preeclampsia-An Integrated Bioinformatical Analysis.
482 Biology (Basel) 9.
483 Nelson, W., Adu-Gyamfi, E.A., Czika, A., Wang, Y.X., Ding, Y.B., 2020. Bisphenol A-induced
484 mechanistic impairment of decidualization. Mol Reprod Dev 87, 837-842.
485 Okae, H., Toh, H., Sato, T., Hiura, H., Takahashi, S., Shirane, K., Kabayama, Y., Suyama, M., Sasaki, H.,
486 Arima, T., 2018. Derivation of Human Trophoblast Stem Cells. Cell Stem Cell 22, 50-63.e56.
487 Papuchova, H., Latos, P.A., 2022. Transcription factor networks in trophoblast development. Cell Mol Life
488 Sci 79, 337.
489 Raguema, N., Moustadraf, S., Bertagnolli, M., 2020. Immune and Apoptosis Mechanisms Regulating
490 Placental Development and Vascularization in Preeclampsia. Front Physiol 11, 98.
491 Roberts, R.M., Ezashi, T., Schulz, L.C., Sugimoto, J., Schust, D.J., Khan, T., Zhou, J., 2021. Syncytins
492 expressed in human placental trophoblast. Placenta 113, 8-14.
493 Rosenfeld, C.S., 2021. Transcriptomics and Other Omics Approaches to Investigate Effects of Xenobiotics
494 on the Placenta. Front Cell Dev Biol 9, 723656.
495 Saha, B., Ganguly, A., Home, P., Bhattacharya, B., Ray, S., Ghosh, A., Rumi, M.A.K., Marsh, C., French,
496 V.A., Gunewardena, S., Paul, S., 2020. TEAD4 ensures postimplantation development by promoting
497 trophoblast self-renewal: An implication in early human pregnancy loss. Proc Natl Acad Sci U S A 117,
498 17864-17875.
499 Sharp, A.N., Heazell, A.E., Crocker, I.P., Mor, G., 2010. Placental apoptosis in health and disease. Am J
500 Reprod Immunol 64, 159-169.
501 Smarr, M.M., Kannan, K., Sun, L., Honda, M., Wang, W., Karthikraj, R., Chen, Z., Weck, J., Buck Louis,
502 G.M., 2018. Preconception seminal plasma concentrations of endocrine disrupting chemicals in relation to
503 semen quality parameters among male partners planning for pregnancy. Environ Res 167, 78-86.
504 Straszewski-Chavez, S.L., Abrahams, V.M., Mor, G., 2005. The role of apoptosis in the regulation of
505 trophoblast survival and differentiation during pregnancy. Endocr Rev 26, 877-897.
506 Ticiani, E., Gingrich, J., Pu, Y., Vettathu, M., Davis, J., Martin, D., Petroff, M.G., Veiga-Lopez, A., 2021.
507 Bisphenol S and Epidermal Growth Factor Receptor Signaling in Human Placental Cytotrophoblasts.
508 Environ Health Perspect 129, 27005.
509 Ticiani, E., Pu, Y., Gingrich, J., Veiga-Lopez, A., 2022. Bisphenol S Impairs Invasion and Proliferation of
510 Extravillous Trophoblasts Cells by Interfering with Epidermal Growth Factor Receptor Signaling. Int J Mol
511 Sci 23.
512 Tomas, S.Z., Prusac, I.K., Roje, D., Tadin, I., 2011. Trophoblast apoptosis in placentas from pregnancies
513 complicated by preeclampsia. Gynecol Obstet Invest 71, 250-255.
514 Turco, M.Y., Gardner, L., Kay, R.G., Hamilton, R.S., Prater, M., Hollinshead, M.S., McWhinnie, A.,
515 Esposito, L., Fernando, R., Skelton, H., Reimann, F., Gribble, F.M., Sharkey, A., Marsh, S.G.E., O'Rahilly,
516 S., Hemberger, M., Burton, G.J., Moffett, A., 2018. Trophoblast organoids as a model for maternal-fetal
517 interactions during human placentation. Nature 564, 263-267.
518 Varberg, K.M., Iqbal, K., Muto, M., Simon, M.E., Scott, R.L., Kozai, K., Choudhury, R.H., Aplin, J.D.,
519 Biswell, R., Gibson, M., Okae, H., Arima, T., Vivian, J.L., Grundberg, E., Soares, M.J., 2021. ASCL2
520 reciprocally controls key trophoblast lineage decisions during hemochorial placenta development. Proc Natl
521 Acad Sci U S A 118.
522 Wu, M., Yan, F., Liu, Q., Liao, G., Shen, Y., Bai, Z., Liu, X., 2023. Effects of Xenobiotic Compounds on
523 Preeclampsia and Potential Mechanisms. Toxics 11.
524 Zhang, X., Li, B.Y., Fu, L.J., Adu-Gyamfi, E.A., Xu, B.R., Liu, T.H., Chen, X.M., Lan, X., Wang, Y.X.,
525 Xu, H.B., Ding, Y.B., 2020. Stomatin-like protein 2 (SLP2) regulates the proliferation and invasion of
526 trophoblast cells by modulating mitochondrial functions. Placenta 100, 13-23.
527 Žalmanová, T., Hošková, K., Prokešová, Š., Nevoral, J., Ješeta, M., Benc, M., Yi, Y.J., Moravec, J.,
528 Močáryová, B., Martínková, S., Fontana, J., Elkalaf, M., Trnka, J., Žáková, J., Petr, J., 2023. The bisphenol
529 S contamination level observed in human follicular fluid affects the development of porcine oocytes. Front
530 Cell Dev Biol 11, 1145182.

Figure 1

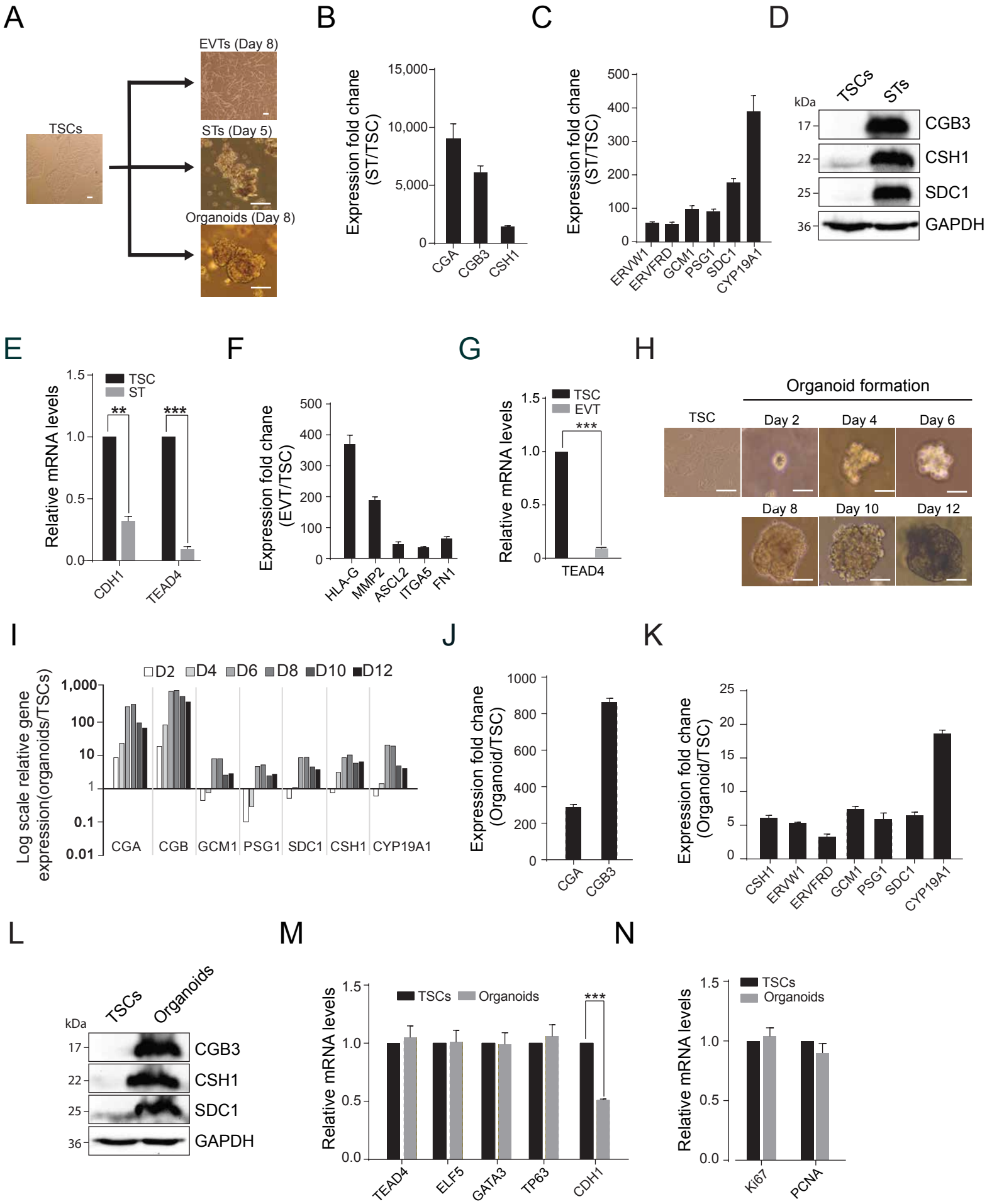
A
TSCs
EVTs (Day 8)
STs (Day 5)
Organoids (Day 8)
B
Expression fold chane (ST/TSC)
15,000
10,000
5,000
0
CGA
CGB3
CSH1
C
Expression fold chane (ST/TSC)
500
400
300
200
100
0
ERVW1
ERVFRD
GCM1
PSG1
SDC1
CYP19A1
D
kDa
TSCs
STs
17
22
25
36
CGB3
CSH1
SDC1
GAPDH
E
Relative mRNA levels
TSC
ST
**
***
1.5
1.0
0.5
0.0
CDH1
TEAD4
F
Expression fold chane (EVT/TSC)
500
400
300
200
100
0
HLA-G
MMP2
ASCL2
ITGA5
FN1
G
Relative mRNA levels
TSC
EVT
***
1.5
1.0
0.5
0
TEAD4
H
Organoid formation
TSC
Day 2
Day 4
Day 6
Day 8
Day 10
Day 12
I
Log scale relative gene expression(organoids/TSCs)
D2
D4
D6
D8
D10
D12
1,000
100
10
1
0.1
0.01
CGA
CGB
GCM1
PSG1
SDC1
CSH1
CYP19A1
J
Expression fold chane (Organoid/TSC)
1000
800
600
400
200
0
CGA
CGB3
K
Expression fold chane (Organoid/TSC)
25
20
15
10
5
0
CSH1
ERVW1
ERVFRD
GCM1
PSG1
SDC1
CYP19A1
L
kDa
TSCs
Organoids
17
22
25
36
CGB3
CSH1
SDC1
GAPDH
M
Relative mRNA levels
TSCs
Organoids
***
1.5
1.0
0.5
0.0
TEAD4
ELF5
GATA3
TP63
CDH1
N
Relative mRNA levels
TSCs
Organoids
1.5
1.0
0.5
0.0
Ki67
PCNA

Figure 2

A

Assessment of BPS impacts on TSC self-renewal

Treatment of TSCs with BPS (0.01, 0.1, and 1 μM) for 2 days

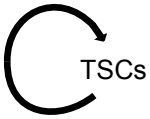

Assessment of BPS impacts on TSC multipotency

Treatment of TSCs with BPS (0.01, 0.1, and 1 μM) during differentiation of TSCs

B

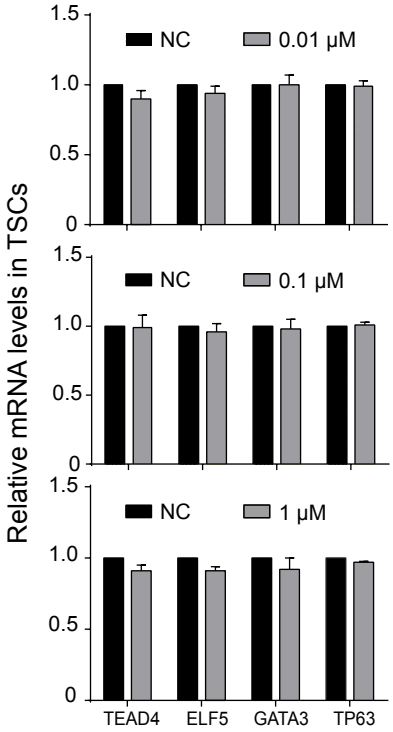

C

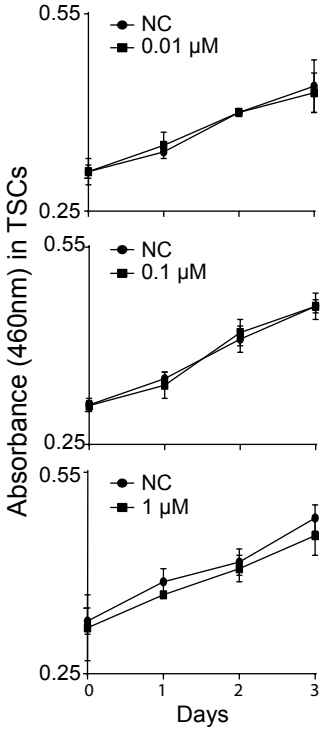

D

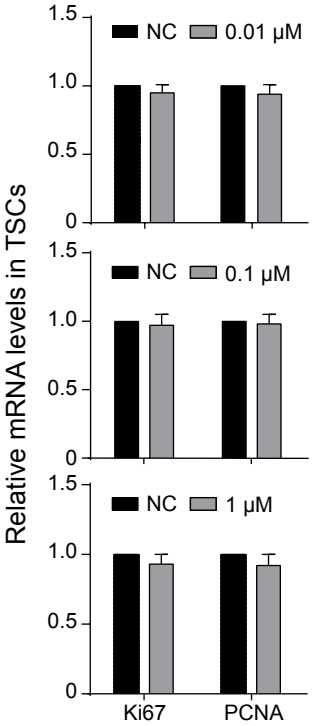

E

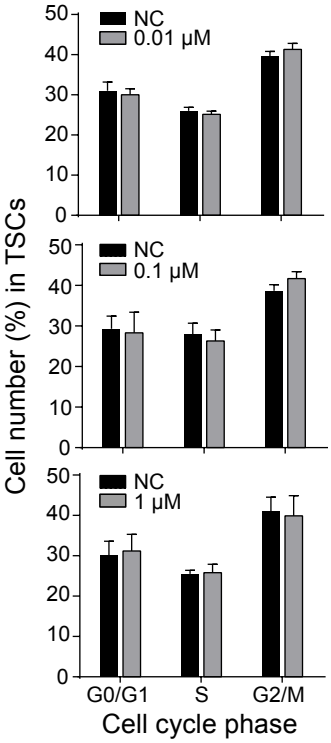

F

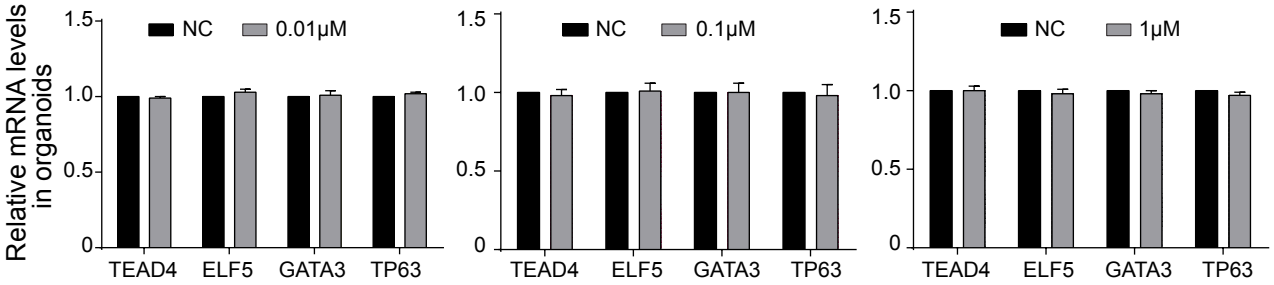

G

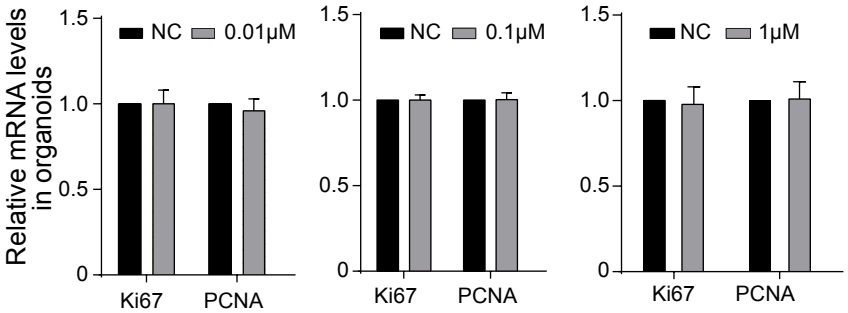

Figure 3

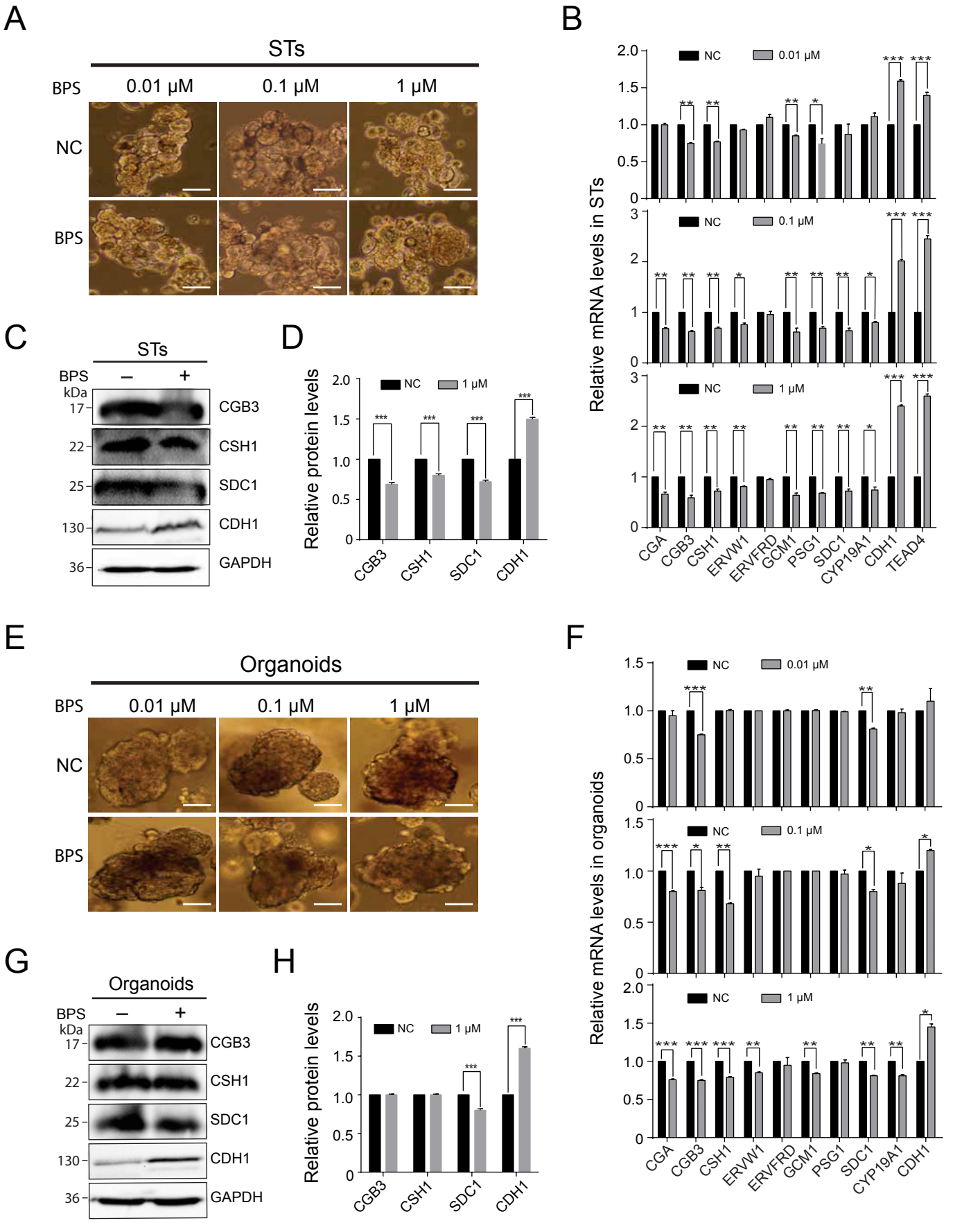
A
STs
BPS
0.01 μM
0.1 μM
1 μM
NC
BPS
B
NC
0.01 μM
0.1 μM
1 μM
Relative mRNA levels in STs
CGA
CGB3
CSH1
ERVW1
ERVFRD
GCM1
PSG1
SDC1
CYP19A1
CDH1
TEAD4
C
STs
BPS
–
+
kDa
17
22
25
130
36
CGB3
CSH1
SDC1
CDH1
GAPDH
D
Relative protein levels
NC
1 μM
CGB3
CSH1
SDC1
CDH1
E
Organoids
BPS
0.01 μM
0.1 μM
1 μM
NC
BPS
F
NC
0.01 μM
0.1 μM
1 μM
Relative mRNA levels in organoids
CGA
CGB3
CSH1
ERVW1
ERVFRD
GCM1
PSG1
SDC1
CYP19A1
CDH1
G
Organoids
BPS
–
+
kDa
17
22
25
130
36
CGB3
CSH1
SDC1
CDH1
GAPDH
H
Relative protein levels
NC
1 μM
CGB3
CSH1
SDC1
CDH1

Figure 4

A

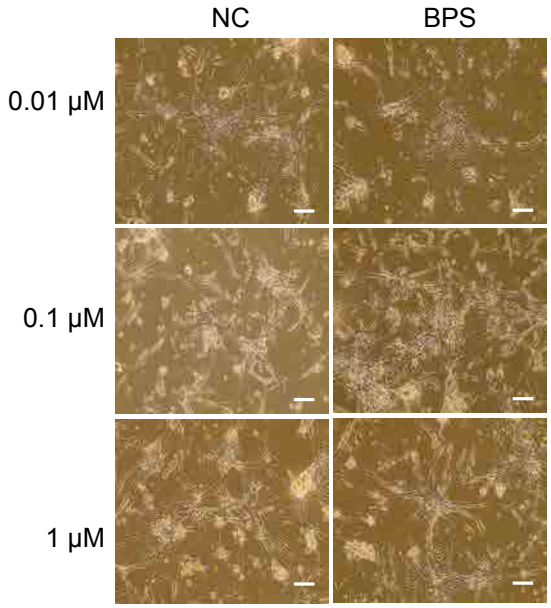
NC
BPS
0.01 μM
0.1 μM
1 μM

B

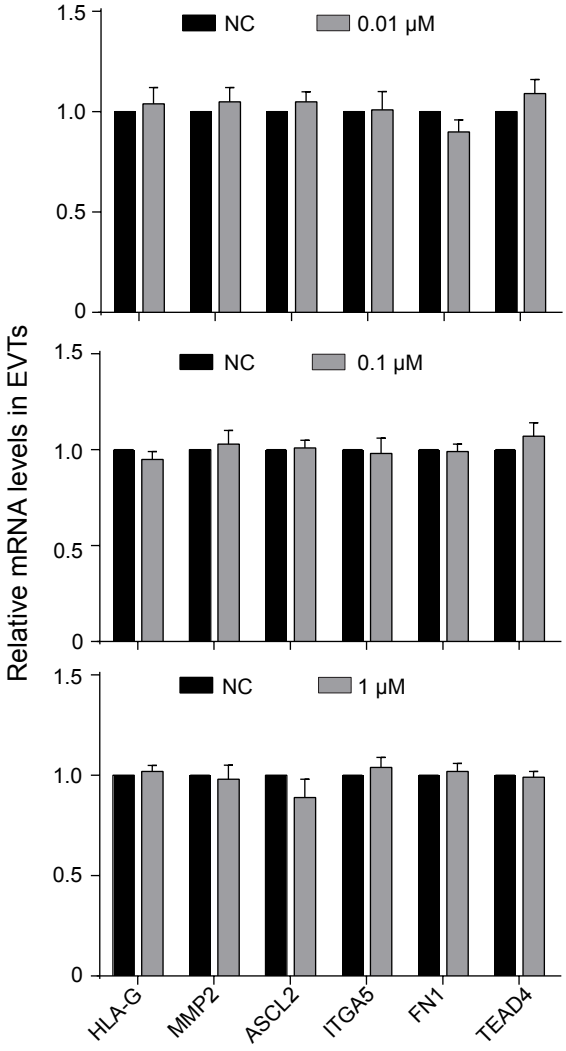
Relative mRNA levels in EVTs
NC
0.01 μM
0.1 μM
1 μM
1.5
1.0
0.5
0
HLA-G
MMP2
ASCL2
ITGA5
FN1
TEAD4

Figure 5

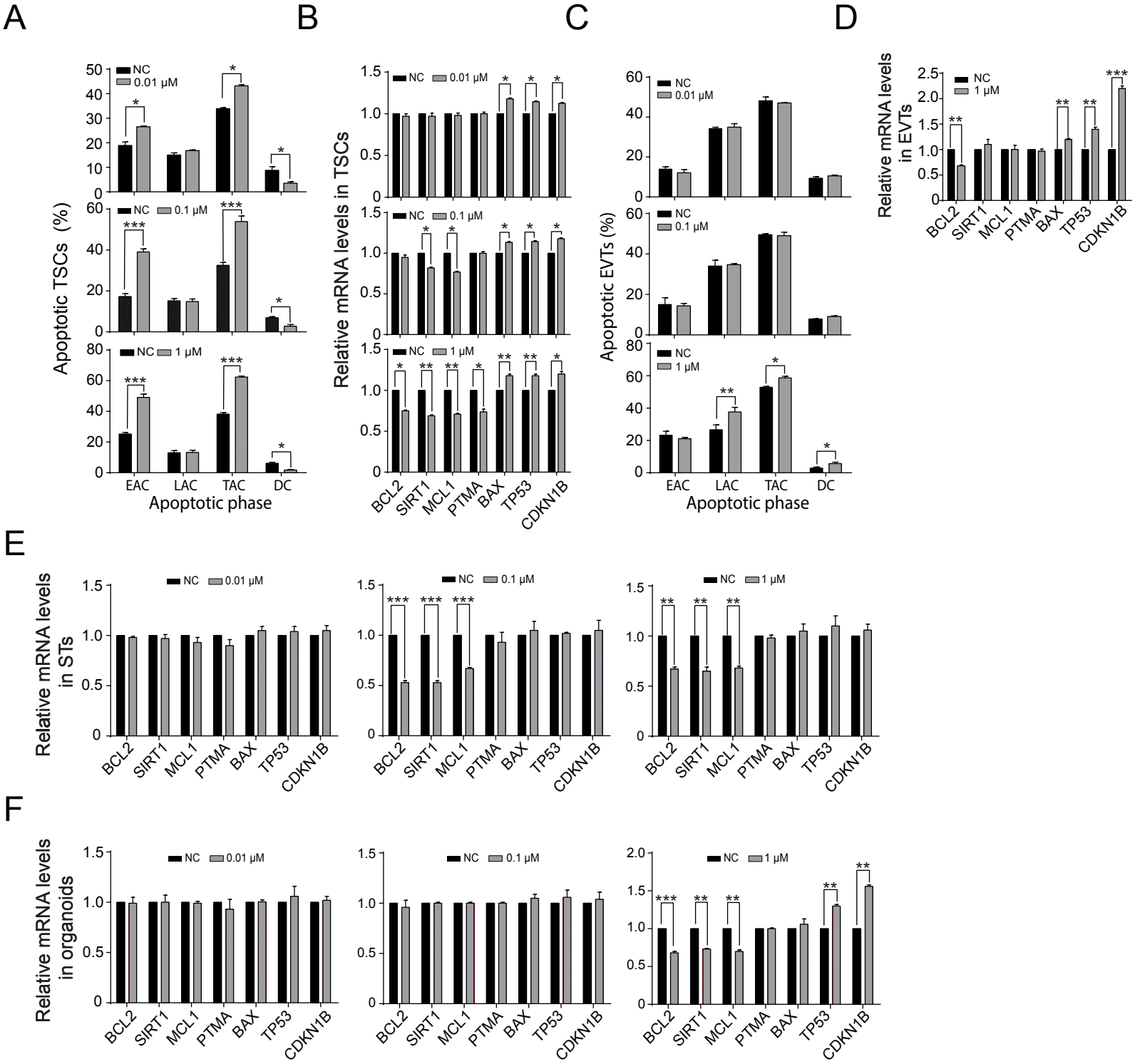
A
B
C
D
E
F
NC
0.01 μM
0.1 μM
1 μM
Apoptotic TSCs (%)
Relative mRNA levels in TSCs
Apoptotic EVTs (%)
Relative mRNA levels in EVTs
EAC
LAC
TAC
DC
Apoptotic phase
BCL2
SIRT1
MCL1
PTMA
BAX
TP53
CDKN1B
Relative mRNA levels in STs
Relative mRNA levels in organoids

Supplementary data

-

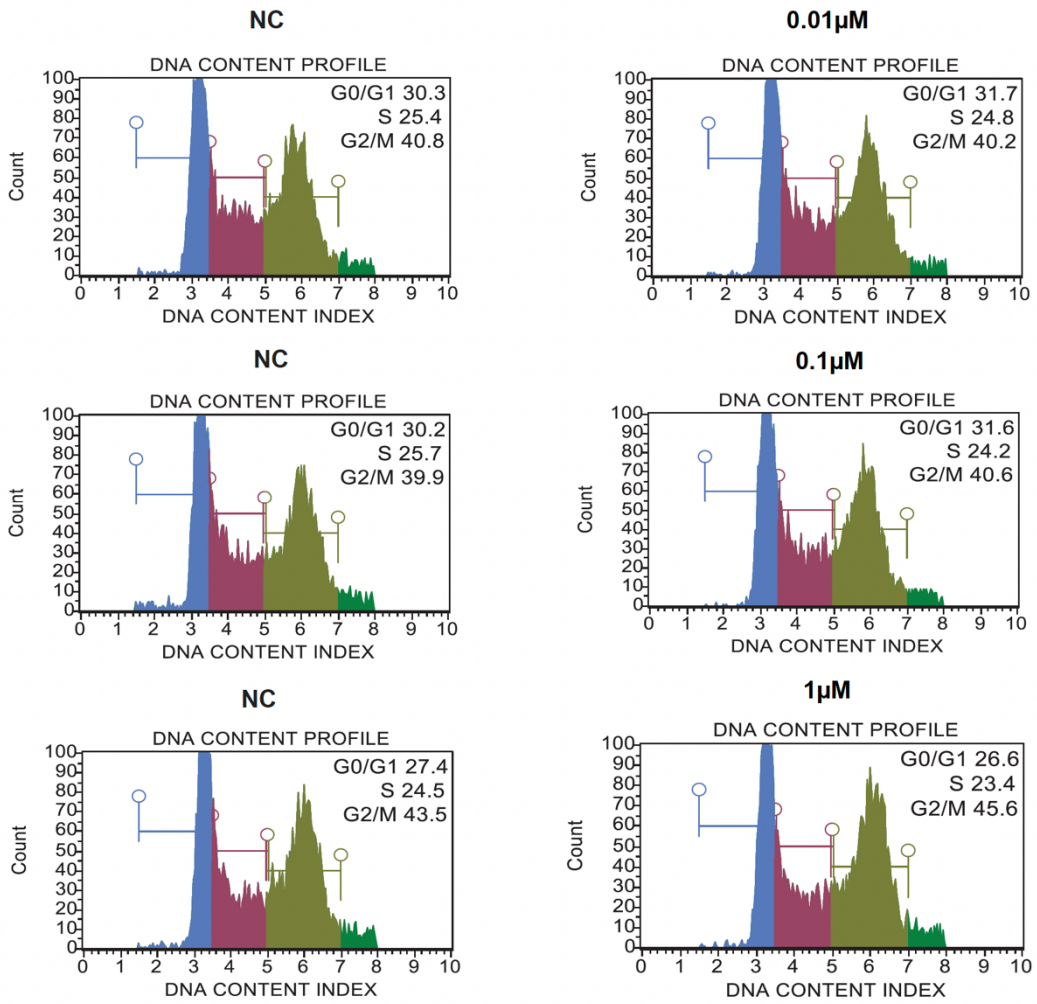

Supplementary Fig.1. Representative histogram from cell cycle analysis presenting the proportion of cells in each phase of the cell cycle.

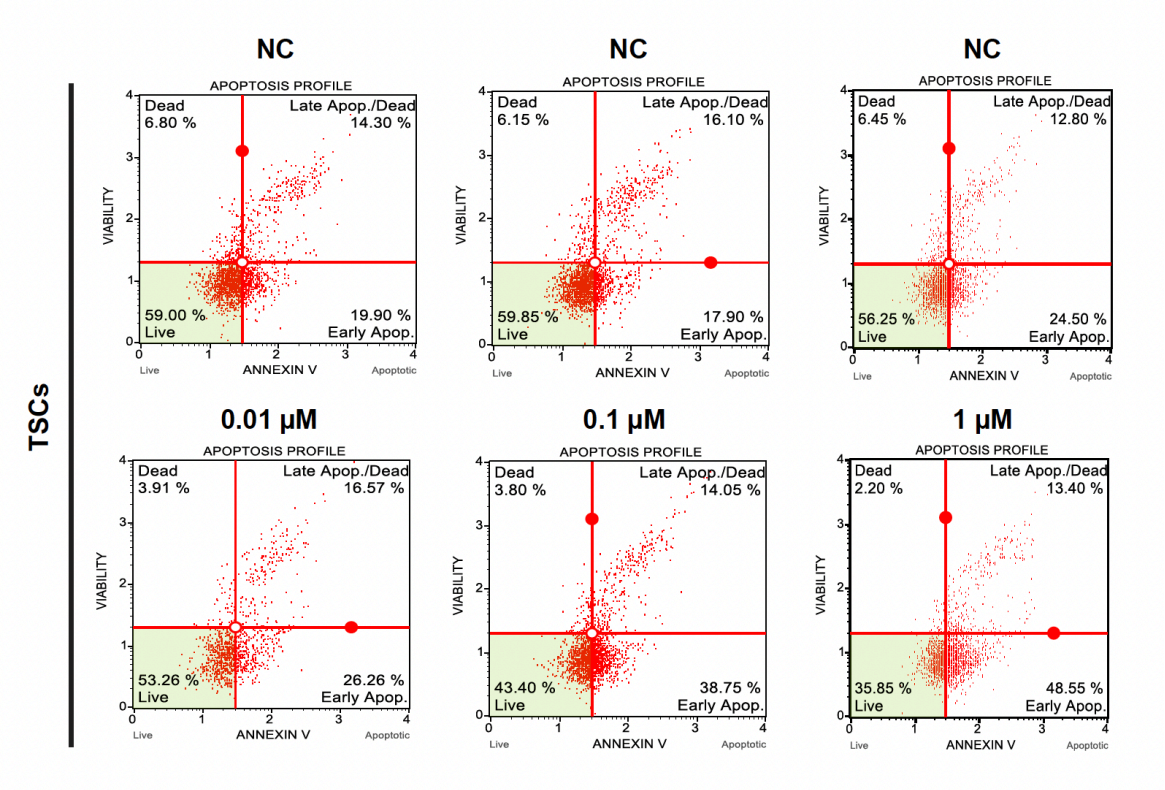

Supplementary Fig. 2. Representative graphs showing the proportion of apoptotic cells among the BPS-treated TSCs and NCs.

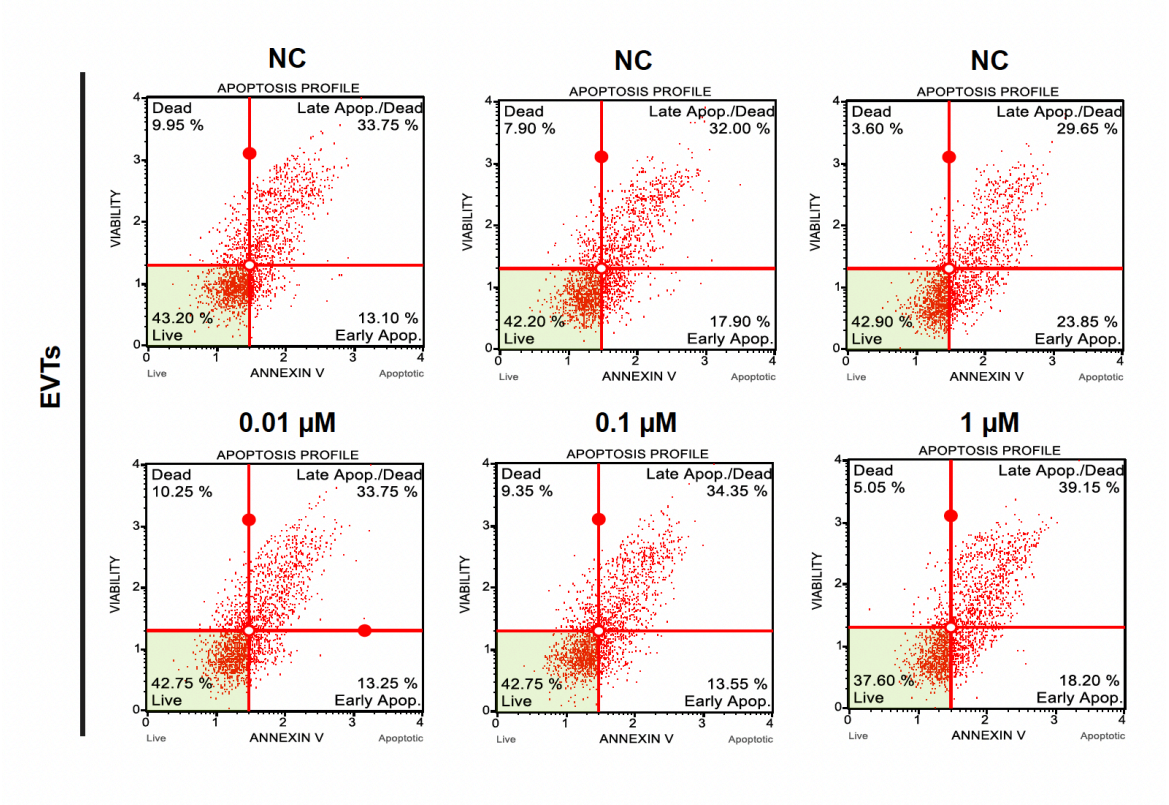

Supplementary Fig. 3. Supplementary Fig.3. Representative graphs showing the proportion of apoptotic cells among the BPS-treated EVTs and NCs.

S

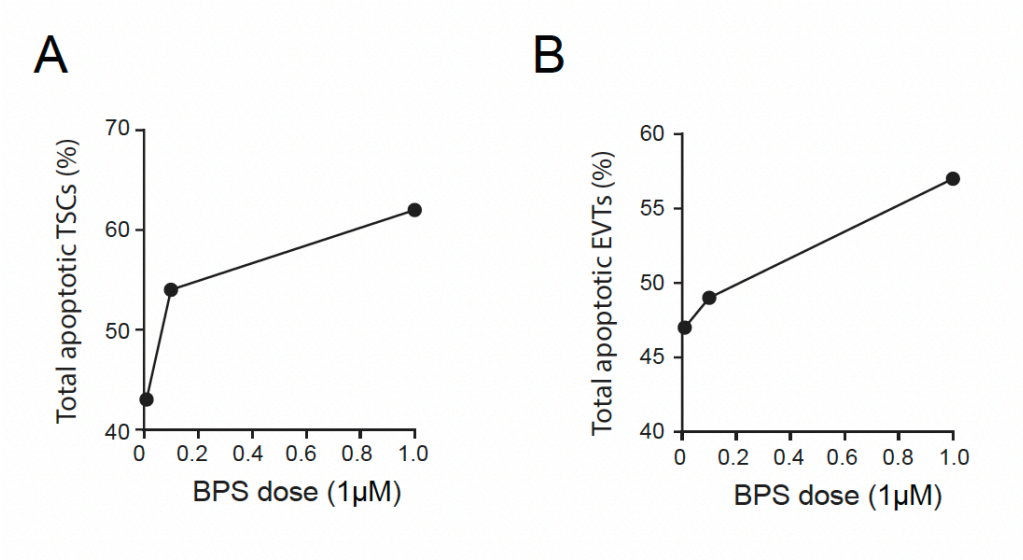

Supplementary Fig. 4. Line graphs showing the dose-dependent relationship between BPS and apoptotic TSCs (A) and EVTs (B).

Supplementary Table 1. A list of primers ued for quantitative PCR	
GAPDH _L	TGACTTCAACAGCGACACCC
GAPDH_R	TTCGTTGTCATACCAGGAAATGAG
CGA _L	GTCCAAAAGAACGTCACCTCA
CGA _R	CGTGTGGTTCTCCACTTTGAA
CGB3_L	GTCAACACCACCATCTGTGC
CGB3_R	GGTAGTTGCACACCACCTGAG
CSH1_L	CAGACCTCCTTCTGCTTCTCA
CSH1_R	GATGCGGAGCAGCTCTAGATT
ERVW-1_L	CAACTGCTATCACTCTGCCAC
ERVW-1_R	TCCAACAGACAGTGACTCCAA
ERVFRD-1_L	GCTGGTTCTCATTCTCACGC
ERVFRD-1_R	GGGGATCCTGTACTTTGGAGC
GCM1_L	GCAAGAAGAGCCATGAAGAAA
GCM1_R	TCCCCTGACTTTGTGTTTCAC
PSG1_L	GGGAGATGATGGGACTAGAGG
PSG1_R	CTGGGATTTAAGTTGCTGCTG
SDC1_L	TGAAGATCAAGATGGCTCTGG
SDC1_R	GGTCTGCTGTGACAAGGTGAT
CYP19A1_L	GACTCGAGTTTTTCCCCAAAC
CYP19A1_R	CGATGTACTTTCCTGCACAGC
CDH-1_L	GAACTAACACACGGGGCGAG
CDH-1_R	TTTGTAGTCACCCACCTCTAAG
TEAD4_L	CTCCACGAAGGTCTGCTCTTT
TEAD4_R	GGATGCGGTAAGAGTAGTGTCC
HLA-G_L	TCCACAGATACCTGGAGAACG
HLA-G_R	AGGGTGGCCTCATAGTCAAAG
MMP2_L	AGCTCCCGGAAAAGATTGAT
MMP2_R	GTGCTGGCTGAGTAGATCCAG
ASCL2 _L	CGTGAAGCTGGTGAACTTGGG
ASCL2 _R	CTCCACCTTGCTCAGCTTCTT
ITGA5_L	CCTGCTGTCCACCATGTCTAT
ITGA5_R	GAGCTGCTGACCTTCCAGAG
FN1_L	TAAGGTTCGGGAAGAGGTTGT
FN1_R	AACTGTGTAGGGGTCAAAGCA
PCNA_F	AGCTCTTCCCTTACGCAAGTCT
PCNA_R	AGGAAAGTCTAGCTGGTTTCGG
Ki67_F	ACAGCAACGACATGAAAACCA
Ki67_R	GCCTCAGTCTTATTTTGGCGT
ELF5 _L	CGGGTGGTTAAATCGGAAGC
ELF5_R	ACCCGCTCCAAAATTCCTGT
GATA3_L	GGGCTCTACTACAAGCTTCAC
GATA3_R	CACTTTTTGGATTTGCTAGAC
TP63_L	AGAAACGAAGATCCCCAGATGA
TP63_R	CTGTTGCTGTTGCCTGTACGTT
BCL2_F	ATGACTGAGTACCTGAACCGG
BCL2_R	GAAATCAAACAGAGGCCGCAT
SIRT1_F	CCTAATAGAGTGGCAAAGGAGC
SIRT1_R	ATATACCTCAGCGCCATGGAA
MCL1_F	GGATGGGTTTGTGGAGTTCTT
MCL1_R	AGATATGCCAAACCAGCTCCT
PTMA_F	AATGAGGAAAATGGGGAGCAG
PTMA_R	CCATCCTCTTCCTCACCATCA
BAX_F	TGTCGCCCTTTTCTACTTTGC
BAX_R	CCAATGTCCAGCCCATGATG
TP53_F	CGAGATGTTCCGAGAGCTGAA
TP53_R	TTTTGGACTTCAGGTGGCTG
CDKN1B_F	AATGCGCAGGAATAAGGAAGC
CDKN1B_R	GAACCGGCATTTGGGGAAC